MDPI

Article

Ventilation Simulation in an Underground Ant Nest Structure of *Camponotus japonicus* Mayr

Guanghong Yang [1], Wei Zhou [2,3,*], Jing Xu [2] , Ming Zeng [4], Shengji Wu [5] and Yijun You [3]

[1] School of Engineering, Cardiff University, Cardiff CF24 3AA, UK
[2] Key Laboratory of Advanced Civil Engineering Materials of Ministry of Education, School of Materials Science and Engineering, Tongji University, Shanghai 200092, China
[3] Shanghai Tongmu Construction Consulting Co., Ltd., Shanghai 200092, China
[4] Department of Geotechnical Engineering, Tongji University, Shanghai 200092, China
[5] Department of Structural Engineering, Tongji University, Shanghai 200092, China
* Correspondence: weizhou_tj@tongji.edu.cn; Tel.: +86-21-35081198

Abstract: Ants are ancient animals on the earth and are known as excellent architects in the animal kingdom. The structure and performance of their nests are full of remarkable mysteries. At present, there are only a limited number of studies on the ventilation performance of underground ant nest structures. In this study, the nests of *Camponotus japonicus* Mayr were collected manually, and a three-dimensional digital model of the ant nest structure was obtained by the method of industrial CT scanning. The ventilation performance of the *Camponotus japonicus* Mayr nest structure was numerically simulated using the finite element analysis software, FLUENT. By changing the air inlet and outlet of the nest, the pressure changes inside the nest and the trajectory of the air flow inside the nest could be calculated and analysed, in order to explore the ventilation characteristics of the underground nest structure during natural ventilation. It was found that the ventilation environment inside the nest was stable, and that the external air flow had little effect on the life of the ants inside the nest.

Keywords: underground ant nest structure; *Camponotus japonicus* Mayr; industrial CT scanning; nest entrance; finite element analysis; structural model; ventilation simulation

1. Introduction

As the number of underground buildings increases, their design, construction and post-use have exposed a number of issues, such as the fact that the interior often requires mechanical equipment such as air conditioners and exhaust fans to be in constant operation, in order to maintain its interior airflow and ensure the exchange of gases between the internal and external environments; consequently, providing such a comfortable environment for people living in underground buildings consumes resources. As such, ventilation is always a key design aspect that must be carefully considered to ensure the thermal comfort of the occupants [1], as well as to decrease the amount of energy required to operate buildings [2]. Since ancient times, architects have drawn inspiration from the natural environment and the most dominant trend in the construction industry is rapidly evolving into a requirement for high performance 'green' or 'sustainable' structures [3]. Architects are now studying the self-organisation of biological processes, in order to reconsider the designs of structures and cities [4], designing buildings that are more in line with the concept of sustainability, to reduce resource consumption and to achieve truly green buildings. Jones and Oldroyd found that most group-living insect species (including some bees and ants) can control the microclimate within their nests to maintain a stable living environment that is not affected by fluctuations in the external environment [5]. Ants, among them, are excellent architects and engineers in the animal kingdom [6], and the architecture and performance of their nests are full of amazing wonders.

Much of the current international research in the field of ant nests has focused on the above-ground nest portion, with the most reported research being on termite mounds. Termite mounds offer climate-controlled microhabitats that protect the creatures from jarring climatic changes, and permit them to communicate with the outside world by exchanging materials, energy and information [7]. After studying the natural ventilation systems that keep termites at a consistent temperature in the African sun, architect Mick Pearce developed the nine-story Eastgate skyscraper in Zimbabwe, which was inspired by the natural world [8–10]. The main contribution of bionic buildings, such as the Eastgate, is the use of natural resources as a source of energy (e.g., wind energy) for energy conversion rather than fossil fuels, which reduces the energy consumption to a certain extent [11,12] and provides a reference for the sustainability of buildings. In addition, the Jean-Marie Tjibaou Cultural Center, created by the world-renowned Italian architect Renzo Piano, has been regarded as "Ecological Architecture" in New Caledonia. This construction is notable for its sustainable ventilation design idea that was inspired by nature, which incorporates ten distinctive shell-like structures for air circulation improvement [13,14]. Further research into the ventilation characteristics of ant nest structures is, therefore, a guide to sustainable building ventilation.

However, the majority of ant nests are located underground, and underground ant nests are the most mysterious place of ants. At present, the number of studies on underground ant nests is relatively limited compared to the investigations of above-ground nests, because underground nests are located in the soil, which is not easy to observe; moreover, most researchers lack the technical tools to visualise the complex structure of underground ant nests in three dimensions, making them more difficult to study than above-ground nests. Most studies of underground ant nests have been characterised from an architectural point of view [15–17], with researchers excavating and casting to obtain structural models of underground ant nests; measuring the size, number and depth of nest chambers; measuring the diameter of the nest entrance and the number of nest entrances; and exploring the architectural function of structural components such as nest entrances, channels and chambers. A natural underground ant nest usually consists of a main nest chamber, and several connecting passages that expand outwards to form a network system that is centred on the nest [18]. Longino [19] studied the nests of two neotropical ant species, and found that they constructed complex nest entrances, placing a circular 'door pebble' at the nest entrance to block the entrances in response to nomadic armies of ants. Excavation is the simplest and first method that has been used by humans to access underground ant nests. For example, Peeters et al. [20] dug a deep trench in front of the nest entrance of the Harpegnathos saltator ant, and excavated it using lateral advancement, measuring and mapping its structural profile without damaging its nest chambers and passages. Currently, perfusion is the method most used by biologists to obtain the structure of subterranean ant nests. Tschinkel [21] used plaster casting to reconstruct adult subterranean nests of nine species of ants in northern Florida, enriching the model of the nest structure. For the observation of the structural features of natural subterranean ant nests, a 3D simulation diagram of the interior structure of the nests was created using frozen CNC milling and digital synthesis [18,22]; however, this method is complex to operate, and the initial workload is high. X-ray tomography (CT) is a new method that has become increasingly popular among biologists in recent years, giving more detailed information about the nest structure than casting, and without destroying the interior of the nest [23]. Halley et al. used X-ray tomography to study the excavation process of Argentine ant nests in the laboratory. Perna et al. [24] used X-ray tomography to map the three-dimensional network of ant nests, and analysed it using graph-theoretic tools, finding that the network topology within the nest offered an excellent compromise between effective connectivity within the nest, and a defence against predator attack. In the absence of technical tools with which to visualise and quantify the properties of complex ant nest structures in three dimensions, these studies are difficult to carry out, and the use of X-ray tomography has led to more in-depth studies of ant nests. However, the ventilation properties inside underground ant nest structures have been poorly investigated.

From the point of view of civil engineering, this study located the nest position of *Camponotus japonicus* Mayr with the trapping method, it shaped the nests using a liquid paraffin infusion, and it obtained a digital three-dimensional model of the ant nest structure via manual excavation, industrial CT scanning and other methods. The reverse engineering software, Geomagic Studio, was used to perform a surface fitting on the industrial CT scan results, in order to obtain an underground ant nest structure model that could be used for a finite element calculation. The finite element analysis software, FLUENT, was used to numerically simulate the ventilation performance of the nest structure. By changing the air inlet and outlet of the ant nest, pressure changes in the nest and the flow trajectory of the gas in the nest were calculated and analysed, then, the ventilation characteristics of subterranean ant nests in their natural state were explored.

2. Materials and Methods

2.1. Collection of Underground Ant Nests

As the *Camponotus japonicus* Mayr nest structure is composed of many nest chambers and intricate channels, the whole nest is situated vertically downward, and the inner layer of the nest chamber is obvious; therefore, the nest structure met the requirements of this study. In addition, *Camponotus japonicus* Mayr is a common ant species in China, and there is little covering near the nest entrance, making it easy to locate the nest; therefore, the nest of *Camponotus japonicus* Mayr was chosen for this study.

Camponotus japonicus Mayr belongs to the Hymenoptera, Formicidae, Camponotus, which is a common species of formicine ant found in open fields in east Asia [25], with a wide distribution in most parts of China. *Camponotus japonicus* Mayr is most active at midday from May to June, and from September to October, showing a unimodal shape; from July to August, with activity peaks from 08:00 to 12:00 and from 14:00 to 16:00, respectively, while it is largely inactive from 12:00 to 14:00, showing a bimodal shape.

The research object of this study was the underground ant nest structure; therefore, the first problem to be solved was to find a means of obtaining a complete underground ant nest model. The ant nest was located underground, which made it difficult to observe and measure; thus, certain methods were needed in order to obtain a nest structure and build a model. This experiment was conducted in October 2020, and the underground ant nest was selected for collection in Huixian City in Henan Province, which is close to the T'ai-hang Mountains and is very rich in ant species. For the field collection, after locating the nest, a syringe was used to fill the nest entrance with liquid paraffin until the syringe could not be pushed and the paraffin spilled out of the nest entrance, then, the injection was stopped, and we waited for the paraffin to solidify. The nest was then dug in a 70 cm deep section, with a 70 cm radius around the entrance of the nest, and a small spatula and brush were used to dig, layer by layer, into the centre of the nest. For the extracted paraffin model of the nest, the surface soil was first cleaned, as shown in Figure 1, and then the relative positions between its sections were recorded so that subsequent computer assembly could be conveniently carried out.

Figure 1. Paraffin ant nest blocks after cleaning.

2.2. 3D Model of Underground Ant Nest Structures

After obtaining the paraffin model of the ant nest, it was necessary to digitise it and build a digital model, in order to carry out finite element numerical simulations. Due to the complex structure of the ant nest model, it was a major challenge to model the nest effectively with the numerical simulations. Industrial CT (industry computerised tomography) is an ultra-high resolution 3D imaging technique that relies heavily on mathematical algorithms for converting X-ray attenuation values into cross-sectional images [26]. Repeatedly scanning multiple sections can yield a sufficient number of tomographic images to reconstruct a three-dimensional image, in accordance with certain algorithms. CT is currently the only technique that can measure the internal and external geometries of a component, without cutting through it and destroying it [27]; therefore, in this study, an industrial CT scan was used to transform a paraffin-cast ant nest model into a computerised 3D model. The YXLON FF35 CT device, a high-precision scanning device that can reach the micron level of accuracy [28], was used for this scan, and the scanning resolution of this subterranean ant nest structure was set to 60 μm. The CT-scanned and spliced STL model of the *Camponotus japonicus* Mayr nest is shown in Figure 2a. It was imported into the Rhino software, and the individual ant channels that were previously broken due to excavation were spliced together via Boolean operations to form a complete nest structure. The model was then idealised in the reverse engineering software, Geomagic Studio, in order to remove the nails from the surface of the model; the smooth ant nest structure was surface fitted and saved in STP format for subsequent import into the finite element software, FLUENT. The 3D model of the *Camponotus japonicus* Mayr nest after idealisation is shown in Figure 2b.
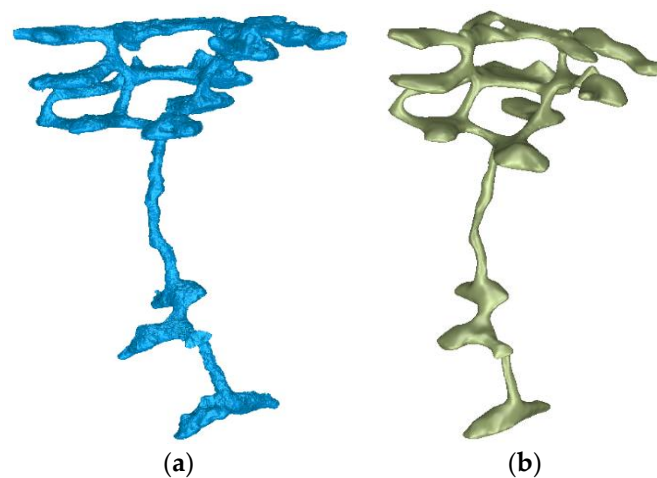

(a)   (b)

Figure 2. *Camponotus japonicus* Mayr nest (**a**) STL model after splicing; (**b**) STP model after idealisation.

2.3. Finite Element Modelling of Underground Ant Nest Structures

CFD (Computational Fluid Dynamics) is the numerical treatment of thermal transfer and fluid dynamics issues that employs two basic computational methods: FEM (finite element methods) and FDM (finite difference methods) [29]. Similar to other finite element software, CFD consists of three modules: pre-processing, solver and post-processing. The pre-processing module is the process of creating the geometric model, setting the boundary conditions, dividing the mesh, selecting the model and setting the convergence conditions. The solver mainly solves the model set in the pre-processing process. The complexity of the model and mesh division, and the performance of the computer, directly determine the length of the calculation time. The post-processing module is used to visualise the results of the solution, such as the velocity, temperature and pressure. This study used FLUENT, a well-known commercial CFD software that has applications in many fields [30], including automotive design, aerospace, etc. The FLUENT software has a rich and reliable set of physical models, such as the often-used standard k-epsilon (k-ε) model, the k-omega (k-ω)

model and the Reynolds stress model (RSM); the user can also set up a turbulence model to suit the needs of the problem being analysed.

In order to obtain a realistic underground nest structure, the solid model of the nest structure that was previously obtained from Geomagic Studio was subtracted from the soil body. Based on the size of the nest structure, the *Camponotus japonicus* Mayr nest was embedded in a 600 mm × 600 mm × 400 mm cube in the Rhino software, and Boolean operations were applied to obtain a true underground nest structure of *Camponotus japonicus* Mayr, which was saved in the SAT format, as shown in Figure 3. This file was then imported into FLUENT, and the individual ant nest structures were presented in the pre-processing module using a volume extraction. There are tetrahedral, hexahedral and prismatic meshes in FLUENT. For an underground ant nest, which is composed of extremely irregular surfaces, an unstructured mesh was chosen for this model, which was more convincing. The total number of cells in the nest structure of *Camponotus japonicus* Mayr was approximately 4.26 million, using a tetrahedral mesh to divide the nest structure. The FLUENT computational physical model of the *Camponotus japonicus* Mayr nest structure and the mesh division of the computational model are shown in Figure 4.
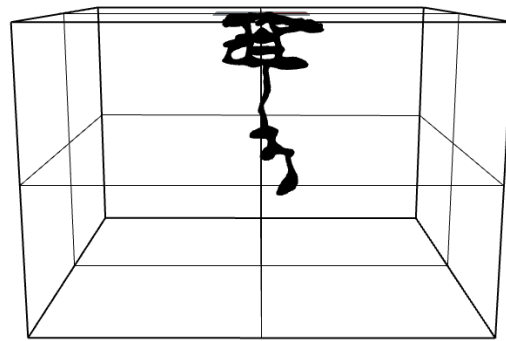

Figure 3. Rhino model of *Camponotus japonicus* Mayr nest in a 600 mm × 600 mm × 400 mm cube.
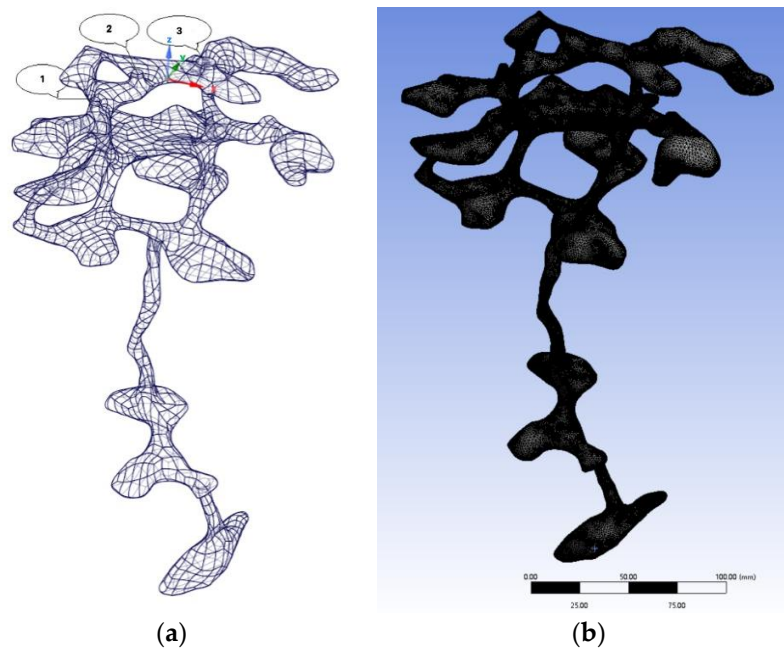

(**a**)　　　　　　　　　　　　(**b**)

Figure 4. (**a**) Physical model and (**b**) mesh division of *Camponotus japonicus* Mayr nest containing nest entrances 1, 2 and 3.

2.4. Ventilation Simulation of Underground Ant Nest Structures

Wind pressure due to the difference in wind speed between the interior and exterior, and thermal pressure due to the difference in temperature between the interior and exterior, were the main causes of air movement. As the gap between the internal temperature of the nest and the soil and external temperature was very small, only natural ventilation under wind pressure was considered in this simulation and it was assumed that no gas exchange took place between the air flowing into the nest structure and the surrounding soil.

As shown in Figure 4a, *Camponotus japonicus* Mayr had three nest entrances; Nest Entrance 2 was located in the middle of the nest; Nest Entrance 1 and Nest Entrance 3 were connected to the downward ant channel, respectively; while Nest Entrance 3 had the largest area. Therefore, in this study, four conditions were chosen for the simulation: Nest Entrance 2, Nest Entrance 3, a combination of both, and two non-adjacent nest entrances, as shown in Table 1.

Table 1. Four conditions for the ventilation simulation of *Camponotus japonicus* Mayr ant nest structures.

Condition	Inlets	Outlets
1	Entrance 2	Entrances 1 and 3
2	Entrance 3	Entrances 1 and 2
3	Entrances 1 and 3	Entrance 2
4	Entrances 2 and 3	Entrance 1

Boundary Conditions and Structural Loadings

This simulation employed the default pressure implicit steady state solver of FLUENT. The coupled velocity and pressure problem was solved using the SIMPLEC algorithm, and the convergence of the residuals and the change in energy and turbulence after each iteration could be clearly seen during the solution. The turbulence model used the standard k-ε model. The energy equation and turbulent dissipation rate equation in a first-order windward discrete format, and the turbulent momentum equation and turbulent kinetic energy equation in a second-order windward discrete format, were used. For the transient analysis, 1000 time steps were set for each condition, with a time step of 0.005 s, i.e., a total physical time of 5 s. During the computational iterations, the turbulent kinetic energy k, turbulent dissipation rate ε and the residuals in the xyz triaxial direction were set to be less than 10^{-5} for convergence in the continuity equation. The initial value of the convergence residuals was set to 10^{-5}. In addition, the boundary conditions were set as follows:

(1)   The inlet boundary was the Velocity-inlet, with the wind direction perpendicular to the inlet surface, and a value of 1 m/s.

(2)   The outlet boundary was set as an outflow, with different FRW values depending on the entrance and exit of the nest.

(3)   The wall boundary was set as a standard wall with no slip and no permeation, i.e., a No Slip Wall.

(4)   Air-liquid was used as the fluid material, and the default values for air were used in the software.

Before starting the calculation, the model was initialised, i.e., given initial values for the flow field, such as the pressure, turbulence coefficient and velocity of the fluid. When calculating, as the number of iteration steps increased, the initial field did not normally have an effect on the final result.

3. Results

In this study, ventilation simulations were carried out for *Camponotus japonicus* Mayr nests in conditions one to four, respectively. As can be seen in Figure 5a, the three nest entrances were almost in a straight line, with the left Nest Entrance 1 and the middle Nest Entrance 2 being of a comparable size; the rightmost Nest Entrance 3 was larger, about twice the size of the other two nest entrances. Nest Entrance 1 and Nest Entrance 3 were

connected to the downward channel, and there were nest chambers on the left and right sides. Nest Entrance 2 was located in the middle, and there was no channel below it; hence, if gas only flowed in through this entrance, it would only flow to the sides.
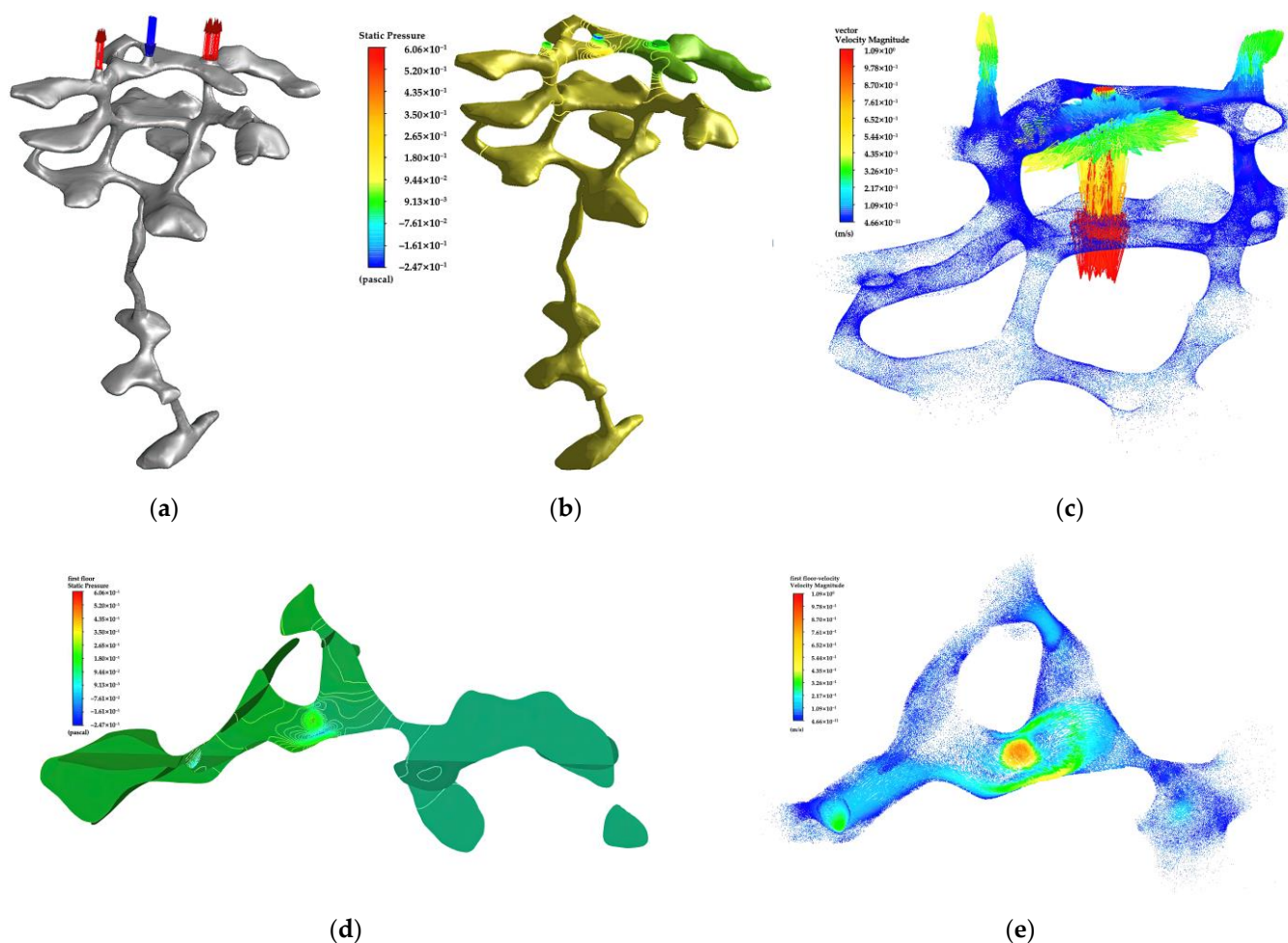

Figure 5. (**a**) Ventilation simulation diagram, (**b**) internal pressure distribution cloud diagram, (**c**) velocity distribution vector diagram, (**d**) pressure distribution on the ground floor and (**e**) wind velocity distribution on the ground floor in condition 1.

3.1. Condition 1: Nest Entrance 2 Was the Inlet, Nest Entrances 1 and 3 Were the Outlets

Condition 1 was an air intake from Nest Entrance 2 in the middle of the *Camponotus japonicus* Mayr nest, whose ventilation simulation cloud diagram is shown in Figure 5. As can be seen from the diagram, when the air was fed into the interior of the nest with a 1 m/s wind, the maximum wind speed inside the nest could reach 4.4 m/s; the gas reached up to the third nest chamber, and as the depth increased, the air flow rate decreased, and the air volume was greatly reduced. The pressure inside the nest became steady, with less pressure on the right side of Nest Entrance 3, where the air could flow out completely due to the larger area of the nest entrance.

3.2. Condition 2: Nest Entrance 3 Was the Inlet, Nest Entrances 1 and 2 Were the Outlets

Condition 2 was an air intake from the largest Nest Entrance 3 on the right side of the *Camponotus japonicus* Mayr nest, whose ventilation simulation cloud diagram is shown in Figure 6. As can be seen from the figure, once a large amount of wind entered the nest, the gas began to flow back and forth, resulting in a higher pressure on the right side of the inlet; meanwhile, the pressure in the area to the left of the two outlets in the first layer was lower, and the pressure inside the other nest layers was stable. Similar to the situation in condition

1, the gas was able to flow to the third layer, and the airflow decreased with an increasing depth. The direction of the gas flow showed that most of the gas flowed from the channel below Nest Entrance 3 to the deeper layers, and then out of the other channels; the pressure and wind velocity were greater at the vertical channels than inside the nest chamber.
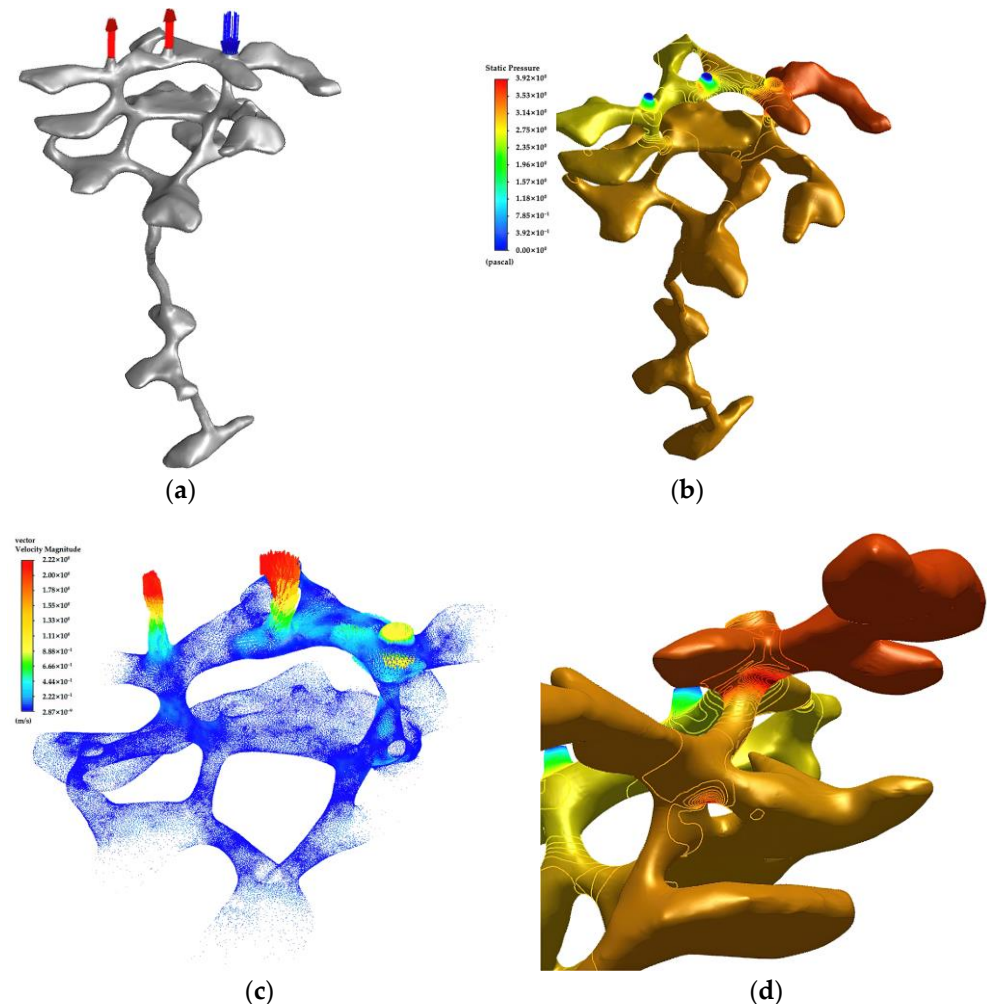

Figure 6. (**a**) Ventilation simulation diagram, (**b**) internal pressure distribution cloud diagram, (**c**) velocity distribution vector diagram and (**d**) pressure diagram of the inlet channel in condition 2.

3.3. Condition 3: Nest Entrances 1 and 3 Were the Inlet, Nest Entrance 2 Was the Outlet

Condition 3 was an air intake from the leftmost Nest Entrance 1 and the largest Nest Entrance 3 on the right side of the *Camponotus japonicus* Mayr nest, whose ventilation simulation cloud diagram is shown in Figure 7. As can be seen from the figure, compared to conditions 1 and 2, there was only one air outlet, resulting in less downward gas flow. Although there was gas flowing into the third layer, the flow rate was very small, and the air was mainly flowing in the first layer; the overall pressure inside the nest chamber was stable and small, and the flow rate was slow; as can be seen from the pressure and velocity vector clouds of the first layer, the air did not flow into the edge area of the nest chamber, and the gas flow became stable after a period of time.
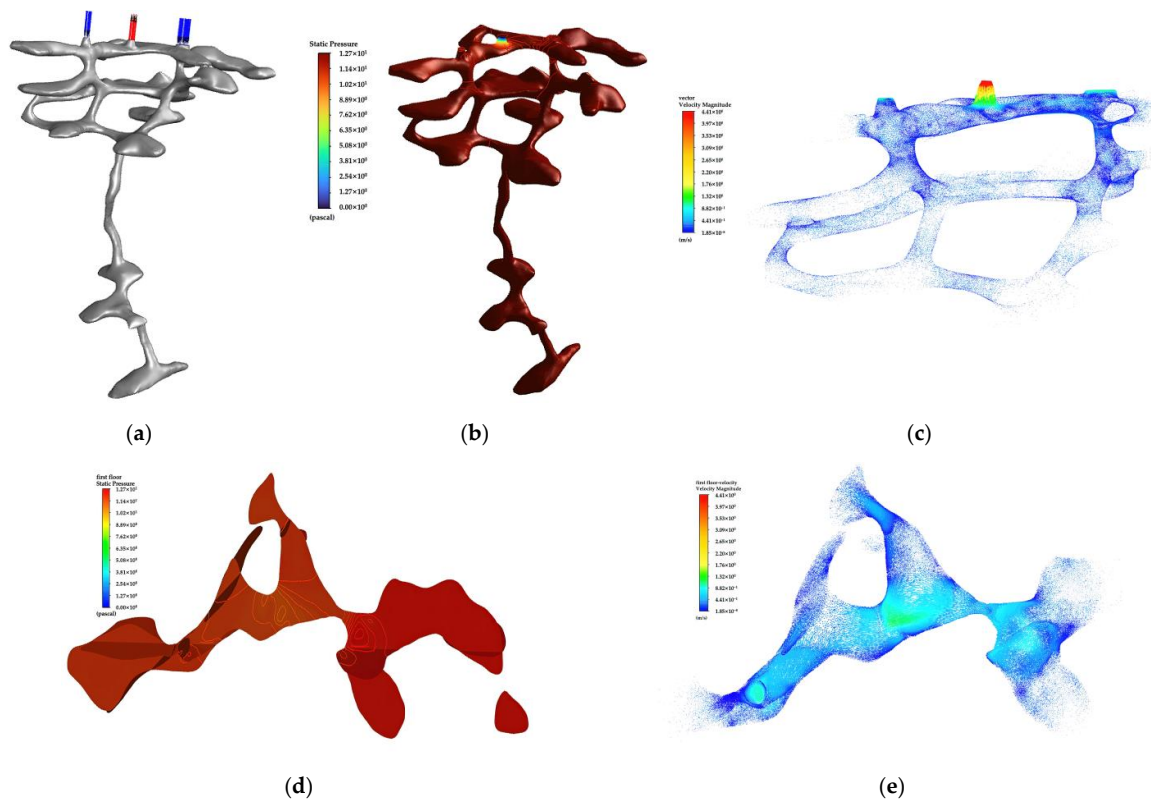
Figure 7. (**a**) Ventilation simulation diagram, (**b**) internal pressure distribution cloud diagram, (**c**) velocity distribution vector diagram, (**d**) pressure distribution on the ground floor and (**e**) wind velocity distribution on the ground floor in condition 3.

3.4. Condition 4: Nest Entrances 2 and 3 Were the Inlet, Nest Entrance 1 Was the Outlet

Condition 4 was an air intake from Nest Entrance 2 in the middle and the largest Nest Entrance 3 on the right side of the *Camponotus japonicus* Mayr nest, whose ventilation simulation cloud diagram is shown in Figure 8. From the pressure distribution cloud and air velocity vector cloud inside the nest, it can be seen that compared to condition 3, the inflow of gas into the downward layer increased, and the flow rate increased because the outlet was located on the leftmost side, and the area was small; the overall pressure inside the nest was stable and the gas flow rate and pressure inside the nest were higher in this condition compared to the other conditions, because the flow rate into the nest was high.
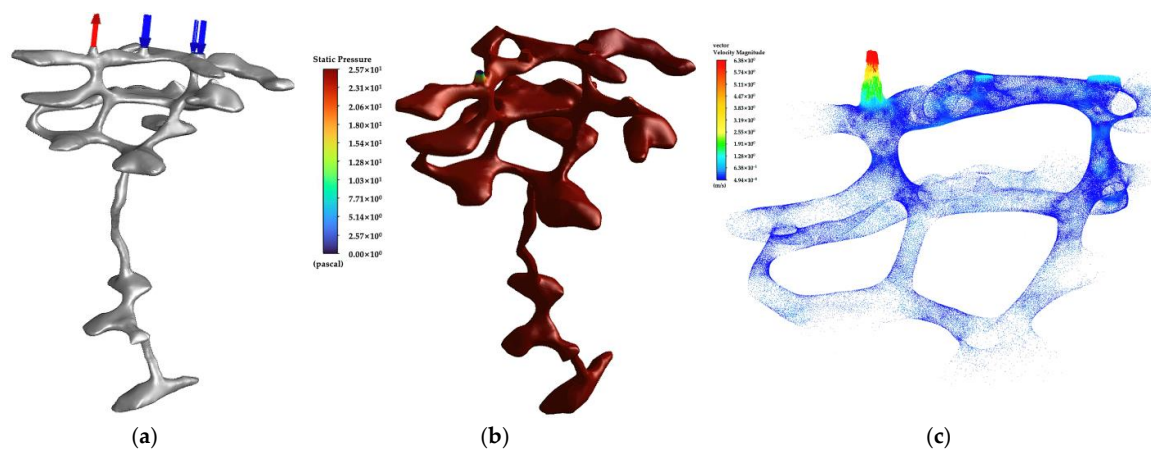

Figure 8. (**a**) Ventilation simulation diagram, (**b**) internal pressure distribution cloud diagram and (**c**) velocity distribution vector diagram in condition 4.

3.5. Analysis of Model Computation Results

The air pressure and velocity of the air flowing through an underground nest is mainly related to the structure and internal shape of the nest. The size of the nest entrance, the relative position of the nest entrance, the amount of air intake and the relationship between the nest entrance and the channel all have an effect on the ventilation. The mean values of pressure in the first layer, the mean values of pressure except for the first layer and the maximum wind velocity in the nest of *Camponotus japonicus* Mayr under the four working conditions are shown in Table 2.

Table 2. Mean pressure and maximum wind velocity inside the ant nest.

Ant Species	Condition	Average Pressure at First Layer (Pa)	Average Pressure Except First Layer (Pa)	Maximum Wind Velocity (m/s)
Camponotus japonicus Mayr	1	0.62	0.11	1.09
	2	3.91	3.21	2.22
	3	12.61	12.05	4.41
	4	25.68	24.88	6.38

The pressure values at all points on the nest structure in the X-Z plane and the pressure values at the inlet and outlet of the nest in the X-Z plane are presented, and the drawn scatter plots are shown in Figures 9–12.
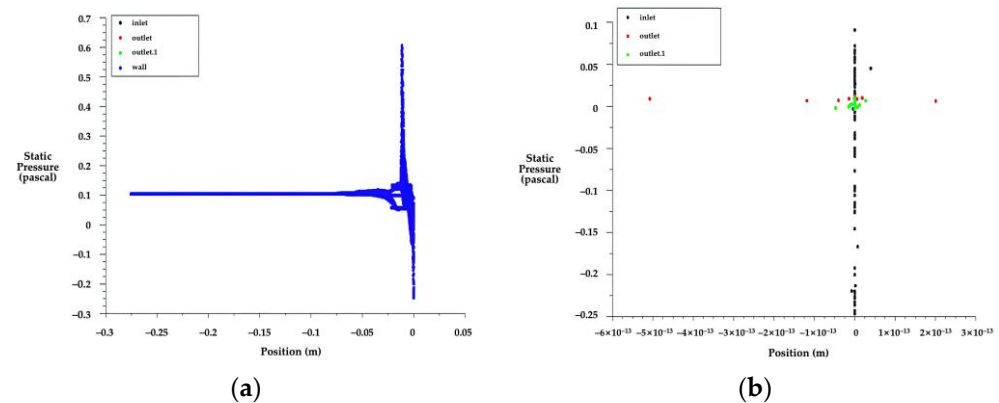

(**a**)

(**b**)

Figure 9. (**a**) Pressure in the X-Z plane and (**b**) inlet and outlet pressure in the X-Z plane of the *Camponotus japonicus* Mayr nest in condition 1.
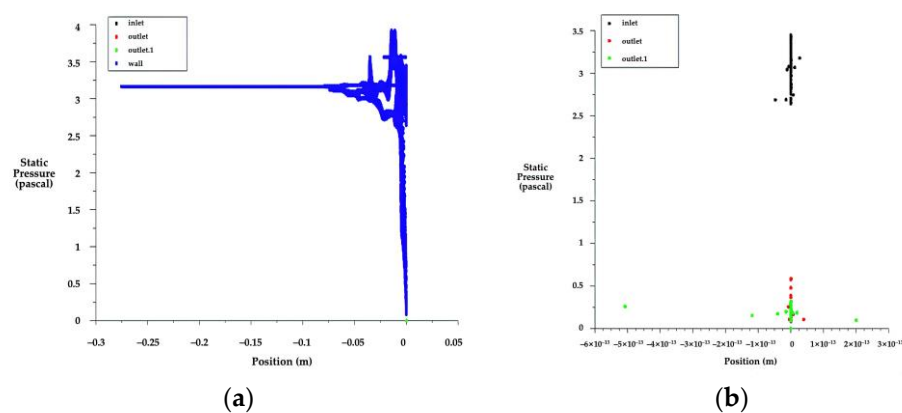

(**a**)

(**b**)

Figure 10. (**a**) Pressure in the X-Z plane and (**b**) inlet and outlet pressure in the X-Z plane of the *Camponotus japonicus* Mayr nest in condition 2.
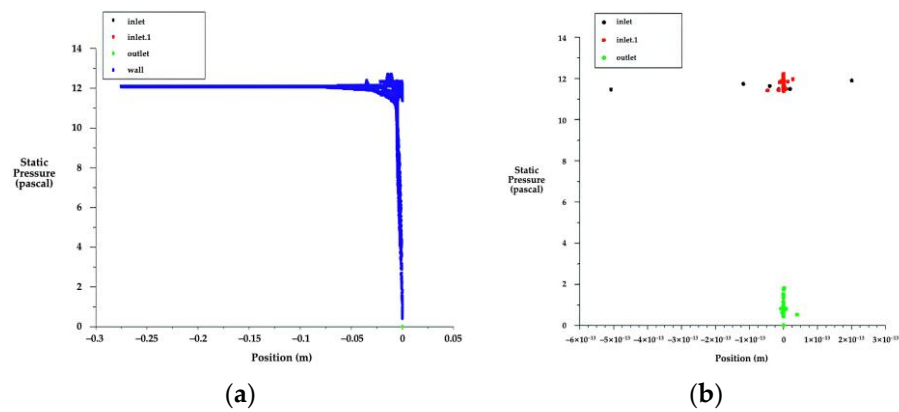
Figure 11. (**a**) Pressure in the X-Z plane and (**b**) inlet and outlet pressure in the X-Z plane of the *Camponotus japonicus* Mayr nest in condition 3.
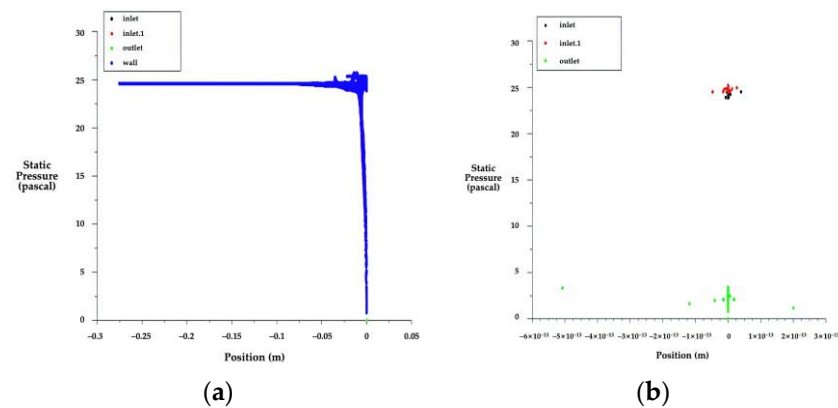

Figure 12. (**a**) Pressure in the X-Z plane and (**b**) inlet and outlet pressure in the X-Z plane of the *Camponotus japonicus* Mayr nest in condition 4.

A wind of 1 m/s flowing vertically into a *Camponotus japonicus* Mayr nest produced too little pressure on the interior of the nest to have an effect on the nest structure. In the case of the same *Camponotus japonicus* Mayr nest, the maximum wind velocity and the trajectory of the gas flow within the nest varied depending on the setting of the air inlet; most nest entrances were connected to the main channel that led to the nest at the deepest level, and some nest entrances were extensions of the main channel, which facilitated the exchange of gas between the nest and the outside world; the pressure values near the air inlet were higher than those near the outlet, and the smaller the inlet, the higher the pressure. In addition, gas did not flow through every layer of the *Camponotus japonicus* Mayr nest; it could flow to the third layer of the nest, mainly because there was gas inside the ant nest itself, and the external gas flowed in when, if there was not enough power and ventilation, it was difficult for the gas to enter the deeper chambers.

For the ventilation simulations of the *Camponotus japonicus* Mayr nest structure from condition 1 to condition 4, it can be seen that the maximum internal pressure values and the maximum air velocity occurred in condition 4, and that both condition 3 and condition 4 had two air inlets, with Nest Entrance 3 being the air inlet. The *Camponotus japonicus* Mayr nest had five levels, the first three of which were approximately the same size and were joined together by two barely misaligned channels. The third layer was connected downwards by a long thin channel that was staggered from the two channels connecting the first three layers; thus, when gas was poured in from the outside, it was difficult for it to flow below the third layer. There was much inflow of gas to the deeper layers in condition 3 because both the inlets were connected to the downward channels, and when gas flowed into the second layer, again because of the irregularity of the nest chamber, some of the gas could flow into the deeper layers.

4. Conclusions

In this study, the underground nest of *Camponotus japonicus* Mayr was taken as an example, and a digital 3D model of the nest structure was obtained through a liquid paraffin infusion, manual excavation and industrial CT scanning. The nest structure of *Camponotus japonicus* Mayr was analysed using the finite element analysis software, FLUENT, in order to explore the special characteristics of the nest structure during ventilation, to explore the potential scientific and engineering value of the nest structure in the field of engineering, and to design a more reasonable structural form to reduce resource consumption and achieve a truly green building. Depending on the selection of the air inlet and outlet, the following conclusions can be drawn:

1. When gas flows in from the nest entrance above the nest channel, the gas can more easily enter deeper into the nest chamber layer than when it flows in from other locations; however, as the depth increases, much less gas flows to the deeper layer.
2. When gas flows in from multiple nest entrances, and out from a small number of nest entrances, gas can enter deeper nest layers due to the increased flow of gas into the nest.
3. When one nest entrance is larger than the others, whether it is the inlet or outlet, the pressure near the nest entrance is lower, and the flow of gas through this nest entrance is slower.
4. When there is no gas exchange between the interior of the nest and the surrounding soil, gas will not flow to the deepest level of the nest, i.e., the queen's chamber, if the nest opening is only at ground level.
5. When the nest is being ventilated, the pressure at the inlet is the highest and the pressure at the outlet is the lowest. Compared to other layers, the pressure at the first layer is also higher, and the ants will often reinforce the nest entrance to prevent it from being damaged and affecting the exchange of gas between the nest and the outside.

As a result, the ventilation inside the underground ant nest is stable, and has little impact on the life inside the underground ant nest, regardless of the changes in external airflow. The purpose of ventilation and air exchange inside the ant nest is mainly achieved through the social self-balance or internal balance among the members of the colony. In addition, the natural ventilation characteristics of the underground ant nest structure are worthy of reference and investigation by human beings so that a suitable indoor environment can be maintained without relying on conventional air-conditioning systems, thus, meeting the requirements of a green building.

5. Future Directions

This study provides implications for sustainable building ventilation through the collection of *Camponotus japonicus* Mayr nests, the innovative use of CT scanning techniques to obtain 3D models of nest structures, and the simulation of their ventilation in the finite element analysis software, FLUENT. Despite the results of this study in terms of the ventilation properties, it is difficult to generalise due to the lack of nest species and numbers studied, in addition to the complexity of natural subterranean nest structures, leaving many areas for further research.

1. The reliability of the simulation results often requires theoretical or experimental results for verification. In this topic, due to the limited literature and experimental conditions available, no experimental verification was carried out for the results of the numerical simulation in this study. In future research, the types and numbers of nests can be increased, and the ventilation characteristics of nest structures can be analysed experimentally or through simulation, and the simulation results can be compared with the results of this project to summarise the more general patterns of underground nest structures.
2. For the ventilation of underground ant nests, this study investigated the ventilation of air from different nest entrances. The effect of temperature inside the nest on

ventilation needs to be further investigated, i.e., the thermal pressure ventilation. For the natural-state ant nest ventilation simulations, pressure clouds and velocity vector diagrams within the nest were used to qualitatively describe the ventilation effect; in subsequent studies, ventilation within the nest structure can be quantitatively analysed.

References

1. Rizal, K.; Ismi, I.; Azli, A.; Izzati, A.; Julaihi, W. A review on Malay vernacular architecture ventilation design elements effectiveness and its application comparative case study: Rumah Kutai Tiang 12 (vernacular) and Rumah Selangorku (contemporary). In *AIP Conference Proceedings*; AIP Publishing LLC: Melville, NY, USA, 2021; p. 020298.
2. Nguyen, T.A.; Aiello, M. Energy intelligent buildings based on user activity: A survey. *Energy Build.* **2013**, *56*, 244–257. [CrossRef]
3. Horman, M.J.; Riley, D.R.; Lapinski, A.R.; Korkmaz, S.; Pulaski, M.H.; Magent, C.S.; Luo, Y.; Harding, N.; Dahl, P.K. Delivering green buildings: Process improvements for sustainable construction. *J. Green Build.* **2006**, *1*, 123–140. [CrossRef]
4. Ireland, T.; Garnier, S. Architecture, space and information in constructions built by humans and social insects: A conceptual review. *Philos. Trans. R. Soc. B Biol. Sci.* **2018**, *373*, 20170244.
5. Jones, J.C.; Oldroyd, B.P. Nest thermoregulation in social insects. *Adv. Insect Physiol.* **2006**, *33*, 153–191.
6. Gadagkar, R. *More Fun than Fun: The Underground Architects and Engineers of the Ant World*; The India Institute of Science: Bangalore, India, 2021.
7. King, H.; Ocko, S.; Mahadevan, L. Termite mounds harness diurnal temperature oscillations for ventilation. *Proc. Natl. Acad. Sci. USA* **2015**, *112*, 11589–11593. [CrossRef]
8. Boroughs, D. Learning from insect engineers. *ASEE Prism* **1999**, *9*, 16.
9. Wolverton, M. Termodynamics. *Mech. Eng.* **2020**, *142*, 43–47. [CrossRef]
10. Turner, J.S.; Soar, R.C. Beyond biomimicry: What termites can tell us about realizing the living building. In Proceedings of the First International Conference on Industrialized, Intelligent Construction at Loughborough University, I3CON. Loughborough, UK; 2008; pp. 1–18.
11. Jiang, Y. Out of the Eastgate. *Build. Sci.* **2011**, *27*, 1–5.
12. Zhao, J.; Xu, Y. Ecological Wisdom Inspired from Termite Mounds—Analysis on Biometric Design of Zimbabwe Eastgate Center. *Build. Sci.* **2010**, *26*, 19–23.
13. Wu, Y.C.; Yang, A.S.; Tseng, L.Y.; Liu, C.L. Myth of ecological architecture designs: Comparison between design concept and computational analysis results of natural-ventilation for Tjibaou Cultural Center in New Caledonia. *Energy Build.* **2011**, *43*, 2788–2797. [CrossRef]
14. Kiroff, L. Why are some designs more interesting than others? The quest for the unusual, the unconventional and the unique in design. In Proceedings of the 2nd International Conference on Structural and Construction Engineering, Rome, Italy, 23–26 September 2003; pp. 1613–1619.
15. Talbot, M.; Kennedy, C.H. The slave-making ant, Formica sanguinea subintegra Emery, its raids, nuptial flights and nest structure. *Ann. Entomol. Soc. Am.* **1940**, *33*, 560–577. [CrossRef]
16. Autuori, M. Contribuição para o conhecimento da saúva (Atta spp.-Hymenoptera-Formicidae). III. Escavação de um sauveiro (Atta sexdens rubropilosa Forel, 1908). *Arq. Inst. Biol.* **1942**, *13*, 137–148.
17. Talbot, M. A comparison of two ants of the genus Formica. *Ecology* **1948**, *29*, 316–325. [CrossRef]
18. Wei, Z.; Wenjun, Q.; Zhi, Z. The preliminary exploration of underground ant nests materials and structure. In Proceedings of the Canadian Society for Civil Engineering Annual Conference 2015: Building on Our Growth Opportunities, Regina, SK, Canada, 27–30 May 2015.
19. Longino, J.T. Complex nesting behavior by two neotropical species of the ant genus Stenamma (Hymenoptera: Formicidae) 1. *Biotropica J. Biol. Conserv.* **2005**, *37*, 670–675. [CrossRef]
20. Peeters, C.; Hölldobler, B.; Moffett, M.; Ali, T.M. "Wall-papering" and elaborate nest architecture in the ponerine antHarpegnathos saltator. *Insectes Sociaux* **1994**, *41*, 211–218. [CrossRef]
21. Tschinkel, W.R. Subterranean ant nests: Trace fossils past and future? *Palaeogeogr. Palaeoclimatol. Palaeoecol.* **2003**, *192*, 321–333. [CrossRef]

22. Qu, W.; Zhou, W.; Zhu, P.; Zhang, Z. Model of Underground Ant Nest Structure Using Static and Dynamic Finite Element Analysis. *Acta Mech. Solida Sin.* **2018**, *31*, 717–730. [CrossRef]

23. Wevers, M.; Nicolaï, B.; Verboven, P.; Swennen, R.; Roels, S.; Verstrynge, E.; Lomov, S.; Kerckhofs, G.; Meerbeek, B.V.; Mavridou, A.M. Applications of CT for non-destructive testing and materials characterization. In *Industrial X-ray Computed Tomography*; Springer: Berlin/Heidelberg, Germany, 2018; pp. 267–331.

24. Perna, A.; Jost, C.; Couturier, E.; Valverde, S.; Douady, S.; Theraulaz, G. The structure of gallery networks in the nests of termite Cubitermes spp. revealed by X-ray tomography. *Naturwissenschaften* **2008**, *95*, 877–884. [CrossRef] [PubMed]

25. Shen, S.; Li, W. Phylogenetic relationship and characterization of the complete mitochondrial genome of Camponotus japonicus (Hymenoptera: Formicoidea: Formicidae). *Mitochondrial DNA Part B* **2022**, *7*, 686–688. [CrossRef]

26. Shepp, L.A.; Kruskal, J.B. Computerized tomography: The new medical X-ray technology. *Am. Math. Mon.* **1978**, *85*, 420–439. [CrossRef]

27. De Chiffre, L.; Carmignato, S.; Kruth, J.-P.; Schmitt, R.; Weckenmann, A. Industrial applications of computed tomography. *CIRP Ann.* **2014**, *63*, 655–677. [CrossRef]

28. Liang, H.; Yang, Y.; Xie, D.; Li, L.; Mao, N.; Wang, C.; Tian, Z.; Jiang, Q.; Shen, L. Trabecular-like Ti-6Al-4V scaffolds for orthopedic: Fabrication by selective laser melting and in vitro biocompatibility. *J. Mater. Sci. Technol.* **2019**, *35*, 1284–1297. [CrossRef]

29. Chung, T.J. *Computational Fluid Dynamics*; Cambridge University Press: Cambridge, UK, 2002.

30. Jeong, W.; Seong, J. Comparison of effects on technical variances of computational fluid dynamics (CFD) software based on finite element and finite volume methods. *Int. J. Mech. Sci.* **2014**, *78*, 19–26. [CrossRef]